

***Morella-rubra-like* metalorganic-framework-derived multilayered $\text{Co}_3\text{O}_4/\text{NiO}/\text{C}$ hybrids
as high-performance anodes for lithium storage**

Yongzhe Wang^a, Mingguang Kong^b, Ziwei Liu^a, Chucheng Lin^a and Yi Zeng^{a}*

a. The State Key Lab of High Performance Ceramics and Superfine Microstructure, Shanghai Institute of Ceramics, Chinese Academy of Sciences, Shanghai 200050, China. *Email: zengyi@mail.sic.ac.cn; Phone and Fax: +86 021 5241 1020

b. Key Laboratory of Materials Physics, Institute of Solid State Physics, Chinese Academy of Science, Hefei, Anhui, 230031, China.

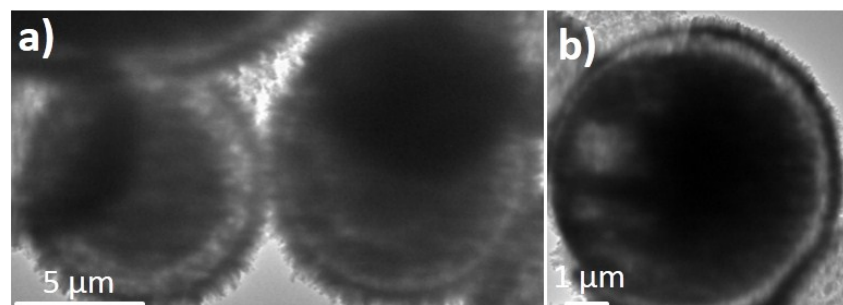


Fig. S1. TEM images of the morella rubra-like CoNi-MOFs.

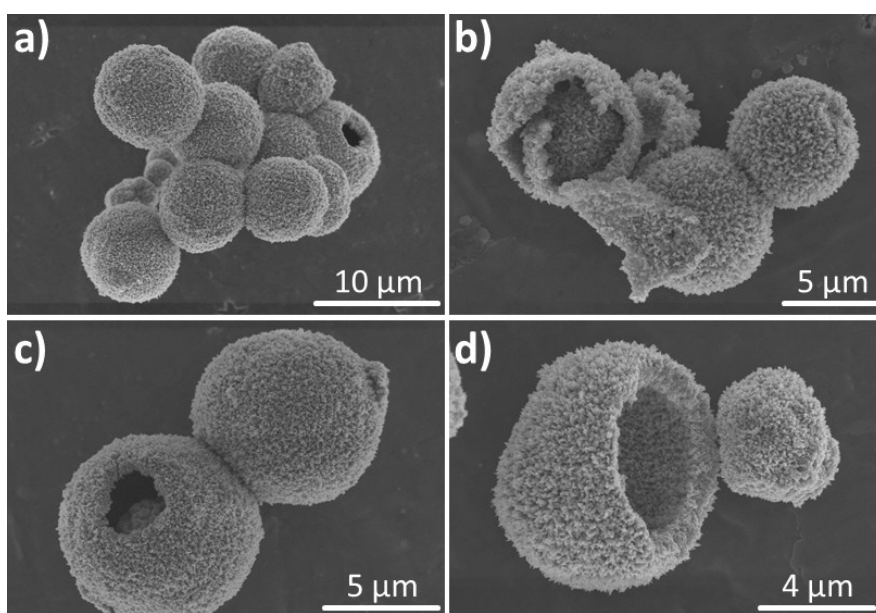


Fig. S2. SEM images of the as-prepared multilayer $\text{Co}_3\text{O}_4/\text{NiO}/\text{C}$ hybrids.

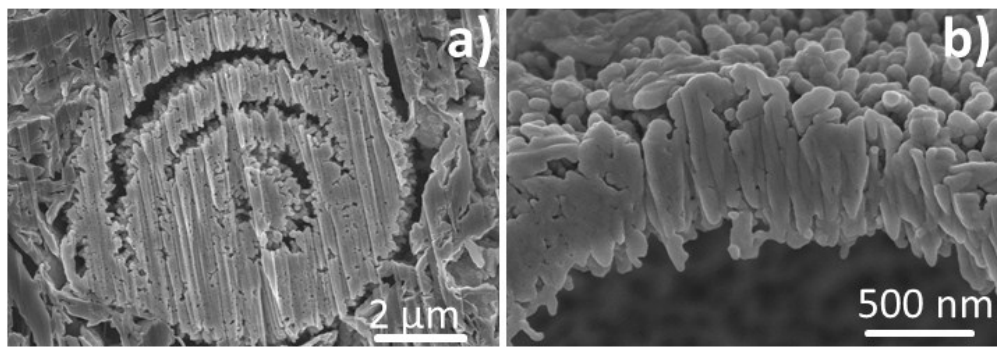


Fig. S3. Cross-section SEM images of the cross section of the multilayer $\text{Co}_3\text{O}_4/\text{NiO}/\text{C}$ hybrids.

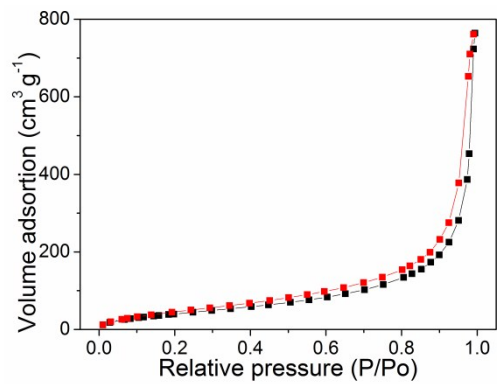


Fig. S4. BET nitrogen adsorption-desorption isotherms of the as-prepared multilayer $\text{Co}_3\text{O}_4/\text{NiO}/\text{C}$ hybrids.

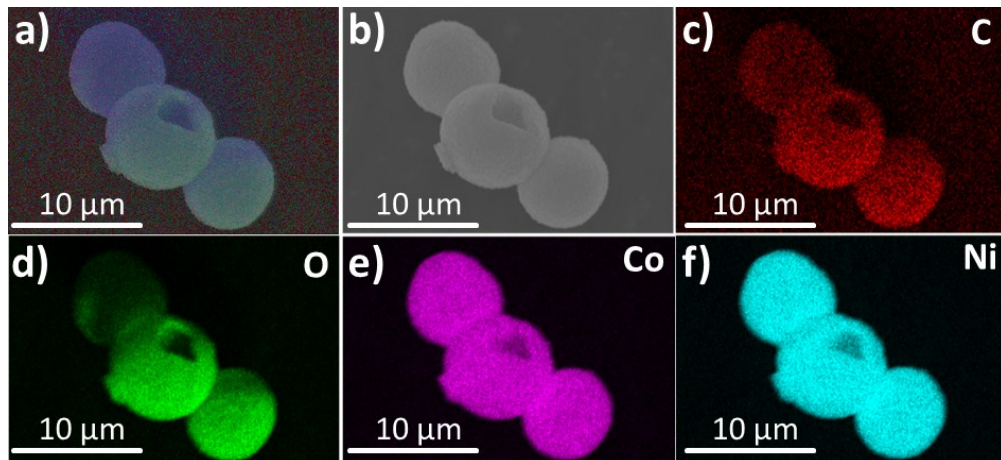


Fig. S5. STEM images of the as-prepared multilayer $\text{Co}_3\text{O}_4/\text{NiO}/\text{C}$ hybrids.

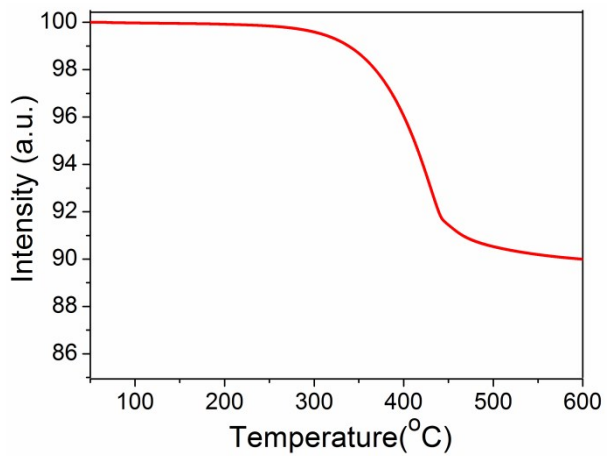


Fig. S6. Thermo-gravimetric analysis (TGA) of the multilayer $\text{Co}_3\text{O}_4/\text{NiO}/\text{C}$ hybrids. The carbon content in the product was identified to be 10 % by weight.

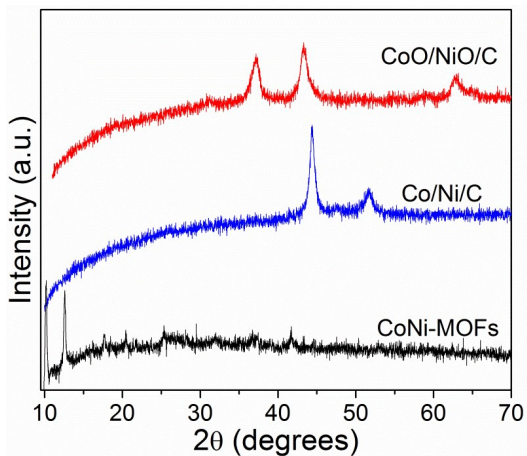


Fig. S7. XRD patterns of the $\text{CoO}/\text{NiO}/\text{C}$ hybrids.

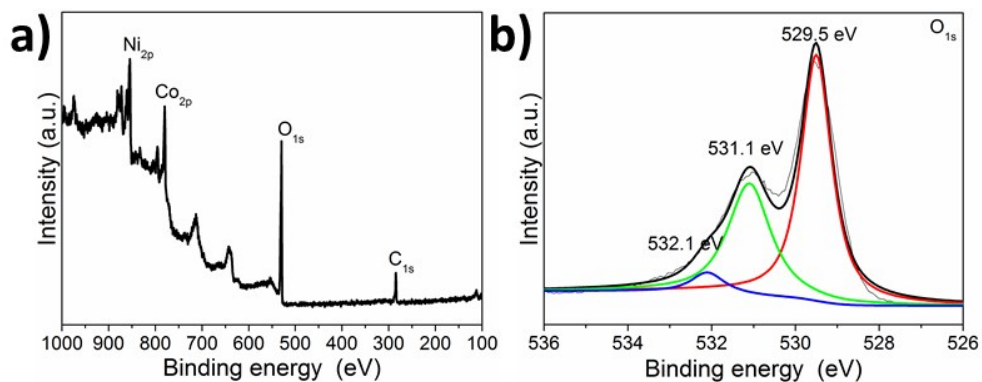


Fig. S8. XPS spectrum of a) the multilayer $\text{Co}_3\text{O}_4/\text{NiO}/\text{C}$ hybrids and b) High-resolution O 1s XPS spectrum of the multilayer $\text{Co}_3\text{O}_4/\text{NiO}/\text{C}$ hybrids.

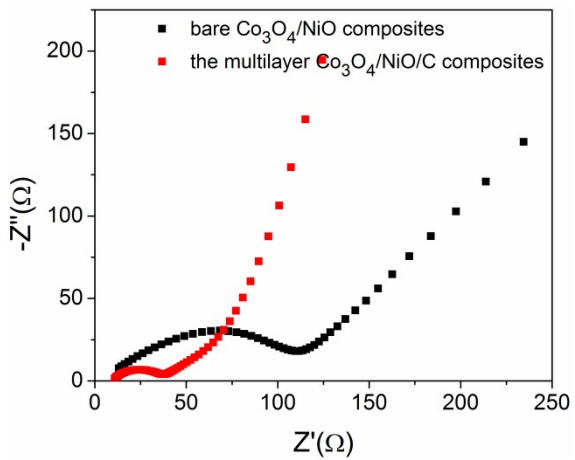


Fig. S9 Nyquist plots of the multilayer $\text{Co}_3\text{O}_4/\text{NiO}/\text{C}$ and bare $\text{Co}_3\text{O}_4/\text{NiO}$ electrodes.

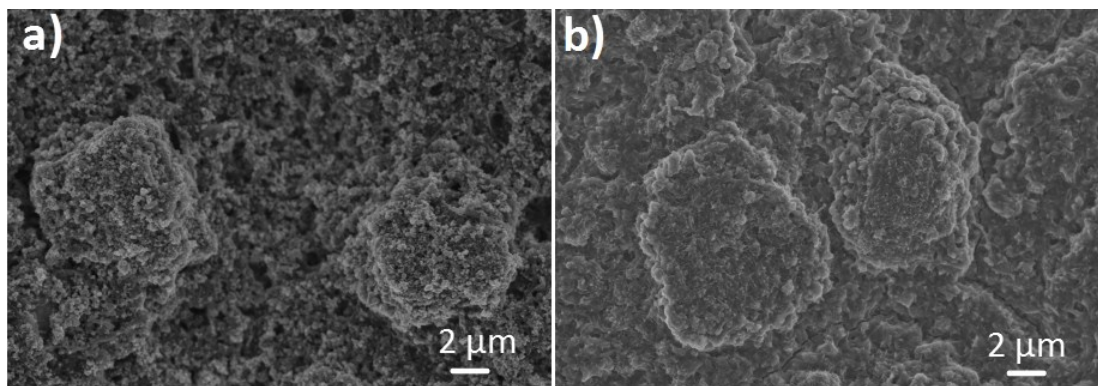


Fig. S10 The SEM image of the multilayer $\text{Co}_3\text{O}_4/\text{NiO}/\text{C}$ electrodes before and after cycling.

Table S1 Comparison of electrochemical performances of the $\text{Co}_3\text{O}_4/\text{NiO}/\text{C}$ electrodes with previously reported Co_3O_4 and/or NiO electrodes.

Electrode materials	Synthetic method	Electrode formulation ^a	Cycling stability (A/B/n) ^b	Ref.
2D-PM NiO	Freeze-drying + annealing	80:10:10	544/200/50	S1
Co_3O_4 -NCNF	Metal nitrate-assisted polymer-blowing	70:20:10	450/5000/500	S2
NiO-NCNF	Metal nitrate-assisted polymer-blowing	70:20:10	420/5000/500	S2
Carbon-doped Co_3O_4	Hydrothermal + annealing	80:10:10	1121/200/100	S3

hollow nanofibers

hollow Co ₃ O ₄ /C	Impregnation-reduction	90:10	880/50/50	S4
Co ₃ O ₄ @CNT	Nanocasting process	85:10:5	700/100/100	S5
H2@Co ₃ O ₄ composite	Hydrothermal + annealing	80:10:10	916/100/100	S6
Co ₃ O ₄ nanosheets/graphene	Hydrothermal + annealing	80:10:10	350/2000/2000	S7
Co ₃ O ₄ /graphene	annealing	80:12:8	525/67/500	S8
Co ₃ O ₄ /rGO aerogel	annealing	60:30:10	935/50/30	S9
Hollow NiO/Ni/G	Hydrothermal + annealing	70:15:15	962/2000/1000	S10
Ni/NiO hybrid	Physical deposition + chemical etching + thermal oxidation	80:10:10	743/1800/900	S11
NiO-S microspheres	chemical solution Method + annealing	80:10:10	739/50/5	S12
NiO/NF	Self-assembly	-:-:-	710/1000/1000	S13
yolk-shell-structured NiO powders	Spray pyrolysis	-:-:-	824/1000/50	S14
the multilayer Co ₃ O ₄ /NiO/C composites	Hydrothermal + annealing	70:20:10	776/1000/1000	This work

a Weight ratio of the active material, carbon and binder. PVDF was used as binder if not mentioned. Other values used were specified.

b A/B/n means the capacity of A (mAh g⁻¹) remained after n cycles at the certain currentdensity of B (mA g⁻¹).

- S1 H. L. Cao, X. F. Zhou, C. Zheng and Z. P. Liu, *ACS Appl. Mater. Interfaces*, 2015, **7**, 11984-11990.
- S2 Y. F. Dong, M. L. Yu, Z. Y. Wang, Y. Liu, X. Z. Wang, Z. B. Zhao and J. S. Qiu, *Adv. Funct. Mater*, 2016, **26**, 7590-7598.
- S3 C. S. Yan, G. Chen, X. Zhou, J. X. Sun and C. D. Lv, *Adv. Funct. Mater*, 2016, **9**, 1428-1436.
- S4 D. L. Wang, Y. C. Yu, H. He, J. Wang, W. D. Zhou and H. D. Abruna, *ACS Nano*, 2015, **9**, 1775-1781.
- S5 D. Gu, W. Li, F. Wang, H. Bongard, B. Spliethoff, W. Schmidt, C. Weidenthaler, Y. Y. Xia, D. Y. Zhao and F. Schuth, *Angew. Chem. Int. Ed.*, 2015, **54**, 7060-7064.
- S6 Y. L. Tan, Q. M. Gao, C. X. Yang, K. Yang, W. Q. Tian and L. H. Zhu, *Sci. Rep.*, 2015, **5**, 12382.
- S7 Y. H. Dou, J. T. Xu, B. Y. Ruan, Q. N. Liu, Y. D. Pan, Z. Q. Sun and S. X. Dou, *Adv. Energy Mater*, 2016, **1501835**, 1-8.
- S8 Z. S. Wu, W. C. Ren, L. Wen, L. B. Gao, J. P. Zhao, Z. P. Chen, G. M. Zhou, F. Li and H. M. Cheng, *ACS Nano*, 2010, **4**, 3187-3194.
- S9 G. B. Zeng, N. Shi, M. Hess, X. Chen, W. Cheng, T.X. Fan and M. N. Derberger, *ACS Nano*, 2015, **9**, 4227-4235.
- S10 F. Zou, Y. M. Chen, K. W. Liu, Z. T. Yu, W. F. Liang, S. M. Bhaway, M. Gao and Y. Zhu, *ACS Nano*, 2016, **10**, 377-386.
- S11 X. L. Sun, W. P. Si, X. H. Liu, J. W. Deng, L. X. Xi, L. F. Liu, C. L. Yan and O. G. Schmidt, *Nano Energy*, 2014, **9**, 168-175.
- S12 J. H. Pan, Q. Z. Huang, Z. Y. Koh, D. N. Neo, X. Z. Wang and Q. Wang, *ACS Appl. Mater. Interfaces*, 2013, **5**, 6292-6299.
- S13 X. F. Zheng, H. E. Wang, C. Wang, Z. Deng, L. H. Chen, Y. Li, T. Hasan and B. L. Su, *Nano Energy*, 2016, **22**, 269-277.
- S14 S. H. Choi and Y. C. Kang, *ACS Appl. Mater. Interfaces*, 2014, **6**, 2312-2316.